Digital Study of The Effect of Radiation on The Flat Solar Collector

Waly Faye[1], Mamadou Seck Gueye[2], Omar Ngor Thiam[1], Aicha Diamanka[2], Mamadou Lamine Sow[1,2]

[1]Fluid Mechanics and Transfer (MFT)Laboratory, Department of Physics, Faculty of Science and Technology, Cheikh Anta DIOP University, Dakar-Fann, Senegal.

[2]Solar Energy and Transfer Research Group (GREST), Faculty of Science and Technology, Cheikh Anta DIOP University (UCAD), Dakar, Senegal.

Corresponding Author: Walyfaye02@gmail.com

Abstract: - This work deals with the numerical study of heat transfer during airflow through a flat plate air thermal solar collector. It consists of the numerical study of the environmental, structural and design parameters that directly influence the operation of this collector. Based on the heat equation, the equations of the different elements of the collector are established. The temperatures of the glass, the absorber and the heat transfer fluid are determined, varying in time and space. The finite difference method was used for the numerical solution. The results obtained allowed us to obtain the desired heat transfer fluid temperature for solar drying of bananas. These results are confirmed by studying the effect of solar radiation on the properties of the glass. For this purpose, the study made for three types of glass (tempered glass, display glass, clear flat glass) allowed to conclude that the clear flat glass of coefficients (2% of absorption and 90% of transmission) is the best choice. The latter gave us the output temperature of the heat transfer fluid for a radiation of 700W/m^2.

Key Words: —*Thermal Transfer, collector, absorption, heat, transmission.*

I. INTRODUCTION

Solar thermal energy is of major importance in the world, because it is clean, renewable and sustainable, and has many practical and industrial applications, including electricity generation, heating, solar collectors and cooling energy systems [1]. Flat plate air collectors convert the solar radiation they receive into usable heat energy. This energy is used in various solar applications, such as food drying, industrial and residential space heating, and solar refrigeration [2].

Collectors for dryers should be made of reliable materials that are corrosion resistant (a life span determinant). The joints securing the collector cover should be strong enough to ensure a reasonably good seal. The collectors could also be equipped with easily removable covers for maintenance.

In this sense, we have seen that a lot of scientific work has been done on good solar collector designs.

The collectors could also be equipped with easily removable covers for maintenance. In this sense, we have seen that a lot of scientific work has been done on good solar collector designs.

M. Baissi et al [2] have carried out work on the modelling of the parameters, related to the operation of the flat plate air collector. The results obtained by comparing two models (the Perrin de Brichambaut model, the Liu and Jordan model) by the daily evolution as a function of true solar time of the outlet temperature of the heat transfer fluid.

The study by Mohamed Yacine NASRI and Azeddine BELHAMRI [3] on the simulation of an indirect solar dryer with forced convection for agro-food products.

Prototype dryer is studied by determining the main characteristics, such as the heating power required for M. Baissi et al [2] have carried out work on the modelling of the parameters, related to the operation of the flat plate air collector. The results obtained by comparing two models (the Perrin de Brichambaut model, the Liu and Jordan model) by the daily evolution as a function of true solar time of the outlet temperature of the heat transfer fluid.

The study by Mohamed Yacine NASRI and Azeddine BELHAMRI [3] on the simulation of an indirect solar dryer with forced convection for agro-food products. These results

prove the increase in air temperature due to the transformation of thermal energy by the effect of solar radiation transmitted through the glass and absorbed by the absorber.

The work of BENKHELFELLAH et al [4] is devoted to the comparative study of the drying kinetics of food products in direct and indirect dryers. For the different temperatures of the dryer elements, the results show that the experimental and theoretical curves converge for a maximum deviation of 10% for the global radiation. They also show that at the absorber, the temperature reaches 110°c while the drying air approaches the value of 90°C.

A. BOULEMTAFES and D. SUMMAR [5], their work aimed at the design and implementation of an indirect solar dryer for agricultural use for drying fruits and vegetables. The dryer consists of a parallelepipedic box, which is supplied with air by a flat solar air collector. The experimental part consisted in studying the characteristics of the drying air when it arrives in the drying box, that is. its temperature, its degree of humidity, its speed and its flow rate as well as their evolution during a characteristic day. The knowledge of the evolution of all these parameters and their interdependencies, allows to select the types of products likely to be dried by this dryer.

A. FERRADJ et al [6] carried out a forced convection solar dryer for drying apricots with the aim of determining the influence of certain parameters on the drying kinetics and quality of these products. For this purpose, they considered it necessary to carry out the following pre-treatments: bleaching, sulphiting and osmotic dehydration. The analysis of variance allowed them to conclude that sulphiting had no influence, whereas bleaching had a very significant effect on weight loss during drying. As for partial osmotic dehydration, it clearly improved the organoleptic quality (texture, colour, taste) of dried apricots. The performance of this drying, the power produced in the collector and its efficiency.

The results obtained showed that the average air temperature at the outlet of the collector is estimated at 46°c. While the air velocity at the outlet of the collector is 2m/s. The airflow required to dry 36kg of apricots for 8 hours, to reduce the moisture content from 86% to 31%, is estimated at 422m³/h. The power required to heat the air is 1.9KW. The source of this energy is the solar collector which produces 27KW. Using the value of the power produced at the collector and the solar irradiation, the efficiency is found to be 11.36%.

In this work, the effect of radiation on the behaviour of the elements of a solar collector is studied numerically using forced convection airflow. For this purpose we will use the finite difference method to solve the governing equations of our geometry model.

II. MATHEMATICAL FORMULATION

A. Geometry Of The Problem

The physical model is presented in Figure 1. The dimensions presented in this work are based on the design data with calculations for the coefficients using mathematical correlations from the literature

The sensor generally consists of :

- a glass pane on the front side ;
- a blackened sheet of metal as an absorber ;
- insulation on the rear and side faces ;
- two conduits with rectangular section

The first duct, located between the glass and the absorber, is the useful duct where the air circulates in forced convection. The second, located below the absorber, is a confined air space.
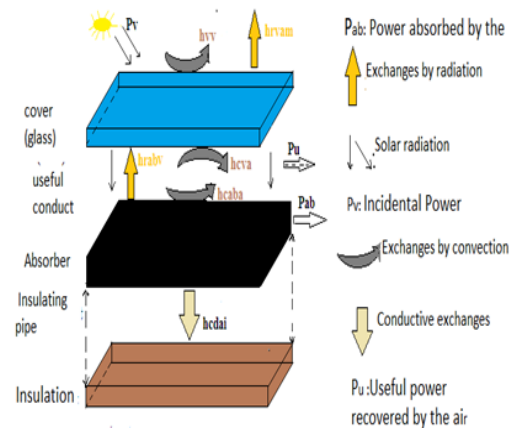

Fig.1.a Normal Collector   1.b Solar dryer

Fig.1.c: The Heat Transfers involved in the collector

B. Simplifying Assumptions

We will consider the following assumptions [8], [9]:

- The airflow is unidirectional (along x),
- The thermal inertia of the heat transfer fluid is neglected,
- The lateral heat losses of the collector are neglected,
- The temperatures of the absorber, the glass and the insulation are uniform in a slice,
- The heat transfer between the insulator and the outside air is neglected.

C. Heat balance equations of the collector

The heat balances of our numerical model are established by taking into account the evolution of the temperatures of all the elements of the collector in time and space. For this purpose, we used the step-by-step nodal method, which consists in cutting the collector into fictitious slices of length ΔX in the direction of the heat transfer fluid flow and writing the balances in each slice using the heat equation [10], [11], [12], [13], [14].

$$m_i Cp_i \frac{\partial T_i}{\partial t} \overrightarrow{V_i \ grad Ti} = \sum h_{ij} \ S_{ij}(T_j - T_i) + \sigma_i$$

(1)

Applying this equation to all the elements of the sensor, we obtain:

➢ *At the level glass pane*

$$\rho_V \ v_v c_{p_v} \frac{dT_v}{dt} = S_c\alpha_v I_g + h_{rvam}S_c(T_{am} - T_v) + h_{VV}S_c(T_{am} - T_v) + h_{Cva}S_c(T_a - T_V) + h_{rabv}S_c(T_{ab} - T_v)$$

(2)

➢ *At the absorber level*

$$\rho_{ab}v_{ab}c_{p_{ab}} \frac{dT_{ab}}{dt} = S_c\alpha_{ab}\tau_v I_g + S_c h_{rabv}(T_v - T_{ab}) + S_c h_{Caba}(T_a - T_{ab}) + S_c h_{Cdai}(T_{am} - T_{ab})$$

(3)

➢ *At the level of the heat transfer fluid*

$$P_u = \ Q_a \ c_{p_a}\Delta x\frac{dT_a}{dx} = h_{cva}S_c(T_v - T_a) + h_{Caba}S_c(T_{ab} - T_a)$$

(4)

D. Dimensionless equations

Characteristic quantities and dimensionless quantities: To obtain dimensionless equations we have used the quantities

L_v is the characteristic length,

$t_{se} = \frac{Q_{se}}{s_c L_C}$: is the reference time of the sensor, and

T_{sc}: is the characteristic temperature of the air leaving the sensor.

$$\widetilde{T_a} = \frac{T_a}{T_{sc}} \ ; \ \widetilde{T_{ab}} = \frac{T_{ab}}{T_{sc}} \ ; \ \widetilde{T_v} = \frac{T_v}{T_{sc}}; \ \tilde{t} = \frac{t}{t_{sc}}; \tilde{x} = \frac{x}{L_c}$$

T_{se}: is again the characteristic temperature of the drying air, which indicates the end of the drying process. The drying time is the total duration of sunlight for which t_{se}=16hours is maintained.

Dimensionless equations:

From these reference quantities, we obtain the following dimensionless equations

➢ *Energy balance at the pane (v)*

$$\frac{d\widetilde{T_v}}{d\tilde{t}} = \ C_4 + C_1\left(\widetilde{T_{am}} - \widetilde{T_v}\right) + C_2\left(T_a - \widetilde{T_v}\right) + C_3\left(T_{ab} - \widetilde{T_v}\right)$$

(5)

$$C_1 = \frac{(h_{rvam} + h_{VV})S_c t_{sc}}{\rho_v v_v \ c_{p_v}}, \widetilde{T_{am}} = \frac{T_a}{T_{sc}},$$

$$C_2 = \frac{h_{Cva}S_c t_{sc}}{\rho_v v_v \ c_{p_v}} \ , \quad C_3 = \frac{h_{rabv}S_c t_{sc}}{\rho_v v_v \ c_{p_v}}, \quad C_4 = \frac{S_c\alpha_v I_g t_{sc}}{T_{sc}\rho_v v_v \ c_{p_v}}$$

➢ *Energy balance at the absorber (ab)*

$$\frac{d\widetilde{T_{ab}}}{d\tilde{t}} = C_8 + C_5\left(\widetilde{T_v} - \widetilde{T_{ab}}\right) + C_6\left(\widetilde{T_a} - \widetilde{T_{ab}}\right) + C_7\left(\widetilde{T_{am}} - \widetilde{T_{ab}}\right)$$

(6)

$$C_5 = \frac{h_{rabv}S_c t_{sc}}{\rho_{ab}v_{ab} \ c_{p_{ab}}}, C_6 = \frac{h_{caba}S_c t_{sc}}{\rho_{ab}v_{ab} \ c_{p_{ab}}},$$

$$C_7 = \frac{h_{cdai}S_c t_{sc}}{\rho_{ab}v_{ab} \ c_{p_{ab}}}, C_8 = \frac{S_c\alpha_{ab}\tau_v I_g t_{sc}}{T_{sc}\rho_{ab}v_{ab} \ c_{p_{ab}}}$$

➢ *Energy balance at the level of the heat transfer fluid (a)*

$$C_9 = \frac{h_{cva}S_c}{\Delta\tilde{x} \ Q_a \ c_{p_a}}, \quad C_{10} = \frac{h_{caba}S_c}{\Delta\tilde{x} \ Q_a \ c_{p_a}}$$

E. Calculation of the collector transfer coefficients

To determine the various heat exchange coefficients "h", the following relationships will be used, depending on whether the transfer is by conduction, convection or radiation.

The coefficients of exchange by convection:

According to the assumptions made, there are two types of convective exchange

Convective exchanges due to the wind: these are the front losses due to the wind noted: h_{VV}. According to the correlation of Hottel and Woertz [7], the coefficient is described according to the following relation:

$$h_{VV} = 5,67 + 3,86_{u_v} \qquad (8)$$

Convective exchange in the collector:

A distinction is made between the exchange coefficient between the absorber and the air (h_{Caba}), and the exchange coefficient between the glass and the air (h_{Cva}).

They can occur either by natural convection (when there is no circulation) or by forced convection. It is written :

$$h_{Cva} = h_{Caba} N_u \frac{\lambda_a}{D_h} \qquad (9)$$

In both cases of convection, various correlations have been developed. For forced convection, and in the case of rectangular ducts, the following expression according to Granier [7] can be used.

$$N_u = 0,0196 R_e^{0,8}. P_r^{1/3} \qquad (10)$$

With $R_e = v. \frac{D_h}{v}$ $v. \rho \frac{D_h}{\mu}$ and $P_r = \mu \frac{c_p}{\lambda}$

Radiation exchange coefficients [8]:

The elements that make up flat plate air collectors (glazing, absorber and insulation) are usually rectangular in shape. All these surfaces are parallel and the distances between them are small. This allows us to simplify the shape factors and take the average temperatures of the elements to express the radiative coefficients. For this purpose, the following classical formulation is often used:

$$h_r = \frac{\sigma(T_1+T_2)(T^2{}_1+T^2{}_2)}{\frac{1-\varepsilon_1}{\varepsilon_1}+\frac{1}{F_{12}}+\frac{1-\varepsilon_2}{\varepsilon_2}\left(\frac{S_1}{S_2}\right)} \qquad (11)$$

The figures 1a, 1b and 1c show the temperature variations of the glass, the absorber and the heat transfer fluid as a function of the displacement at the entrance (fig. 1a), in the middle (fig. 1b) and at the

$$\frac{d\widetilde{T_a}}{d\tilde{x}} = C_9(\widetilde{T_v} - \widetilde{T_a}) + C_{10}(\widetilde{T_{ab}} - \widetilde{T_a}) \qquad (7)$$

Radiative exchange between the glass pane and the surrounding environment:

The relation gives this exchange coefficient

$$h_{rvam} = \sigma \varepsilon_V \frac{(1-\cos\alpha)}{2} (T_V + T_{am})(T^2{}_V + T^2{}_{am})$$

$$(12)$$

Radiative exchange between the glass and the absorber:

$$h_{rabv} = \frac{\sigma(T_V+T_{ab})(T^2{}_V+T^2{}_{ab})}{\frac{1}{\varepsilon_V}+\frac{1}{\varepsilon_{ab}}-1} \qquad (13)$$

Exchanges by conduction:

For our case we will take into account the losses by condition between the absorber and the insulator

$$h_{dabi} = \frac{e_{ab}}{\lambda_{ab}} + \frac{e_{air}}{\lambda_{air}} + \frac{e_{is}}{\lambda_{is}} \qquad (14)$$

Numerical Procedure [9], [15], [16]:

The heat transfer equations (5) (6) and (7) described are non-linear coupled partial differential equations. Due to their complexity, these equations are solved by numerical techniques. The spatial discretization is done by a finite difference method while a purely implicit scheme is adopted for the temporal discretization [15]. The discretized equations according to their level are :

➤ *Energy balance at the level of the window (v)*

$$\frac{\widetilde{T}^t_{v(i)} - \widetilde{T}^{t-\Delta t}_{v(i)}}{\Delta \tilde{t}} = C_4 + C_1(\widetilde{T}_{am} - \widetilde{T}^t_{v(i)}) + C_2(\widetilde{T}^t_{a(i)} - \widetilde{T}^t_{v(i)}) + C_3(\widetilde{T}^t_{ab(i)} - \widetilde{T}^t_{v(i)}) \qquad (15)$$

➤ *Energy balance at the absorber (ab)*

$$\frac{\widetilde{T}^t_{ab(i)} - \widetilde{T}^{t-\Delta t}_{ab(i)}}{\Delta \tilde{t}} = C_8 + C_5(\widetilde{T}^t_{v(i)} - \widetilde{T}^t_{ab(i)}) + C_6(\widetilde{T}^t_{a(i)} - \widetilde{T}^t_{ab(i)}) + C_7(\widetilde{T}_{am} - \widetilde{T}^t_{ab(i)}) \qquad (16)$$

➤ *Energy balance at the level of the heat transfer fluid (a)*

$$\frac{\widetilde{T}^t_{a(i)} - \widetilde{T}^t_{a(i-1)}}{\Delta \widetilde{X}} = C_9(\widetilde{T}^t_{v(i)} - \widetilde{T}^t_{a(i)}) + C_{10}(\widetilde{T}^t_{ab(i)} - \widetilde{T}^t_{a(i)})$$

$$(17)$$

The iterative process is repeated until there is no significant change in the value of T with respect to the following convergence criterion: $\frac{\sum|T^{n+1}-T^n|}{\sum|T^{n+1}|} \leq \varepsilon_r$ with $\mathcal{E}_r$ with is the calculation accuracy.

III. RESULTS AND DISCUSSIONS

After writing the transfer equations and presenting a numerical solution scheme, we will analyse results from our different studies, which mainly concern the evaluation of the temperature in different levels of our flat plate solar collector as a function of time and solar radiation exit (fig. 1c) for an irradiation of 500W.m^{-2}, for which the characteristics of the glass are: transmission 82% and absorption 3%, emissivity 85% and thickness 10mm.

The figure 1a (first instant), figure 1b (mid-instant), and figure 1c (last instant) show us the variations of the temperatures of the different elements of the sensor according to the slices (displacement). At the first two slices, we can see that there is no variation between the air and the glass. This is due to the fact that the air has not yet been in the sensor for a considerable time. So, at the last one, there is a difference in the temperatures between the different parameters of the sensor. At these positions the air has had time to warm up gradually.

To achieve the desired output temperature in a sensor, it is essential to take into account the residence time of the air in the sensor, which is a function of the sensor dimensions.

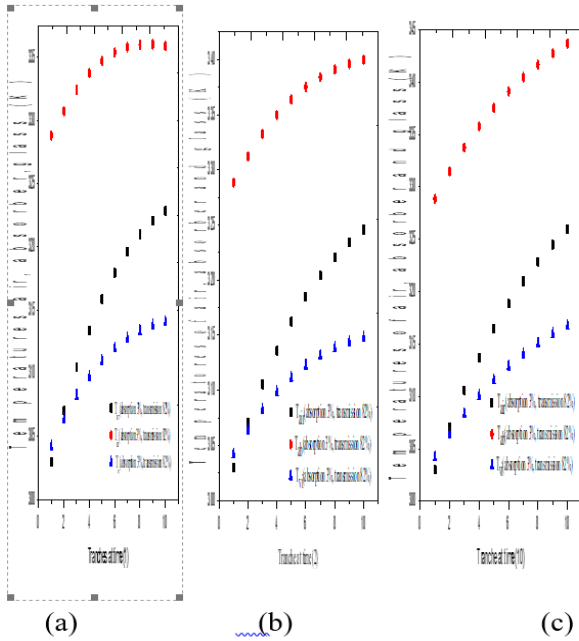(a)   (b)   (c)

Fig.1. Evolution of the temperatures of the glass, the absorber and the heat transfer fluid according to the slices at different times

The figure 2 shows the evolution of the temperature of the outlet fluid as the absorption rate of the glass is increased or decreased for an irradiance of 500W.m^{-2}. The figure 2a shows that whatever the characteristics of the glass, the temperature of the air at the first slice is the same. The figures 2b and 2c : when the absorption coefficient of the glass is low, the differentiation comes from the transmission coefficient, but if the absorption coefficient is not low, the impact on the temperature rise of the heat transfer air is felt.

The choice of glass will be based more on its high absorption coefficient, as this glass will raise the temperature of the heat transfer air in the collector by releasing the heat absorbed by conduction.

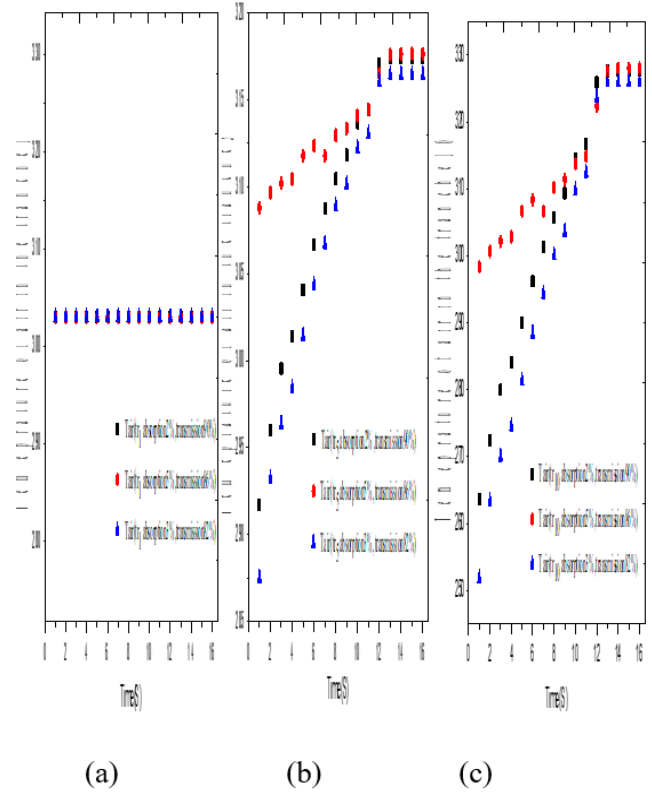(a)   (b)   (c)

Fig.2. Evolution of the collector outlet air temperature as a function of time according to the variations of the absorption rate

The figure 3a shows two phases of evolution of the absorber temperature as a function of the glass characteristics. Between 0 and 8 (dimensionless time), the configuration with the pane of higher absorption coefficient (5%) gives the best temperature of the absorber. In addition to the amount of heat transferred to the absorber, the pane also transfers heat by radiation. In this phase, the effect of the absorption of the pane dominates over the effect of its transmission.

In the second phase, the After a certain time, the temperature of the different panes equilibrates with the temperature of the incident rays. Hence the effect of the absorption is zero. Thus the pane with a transmission coefficient of 90% has the greatest effect on the temperature of the absorber.

The figures. 3b and 3c still confirm that at the beginning of the phase the absorption dominates the transmission. This domination is explained by the effect of the ambient air flow on the absorber. This effect decreases greatly in the second phase, so that a slight difference is observed in the middle and at the outlet of the collector. The air temperature is closer to the absorber temperature at the fifth and tenth stage
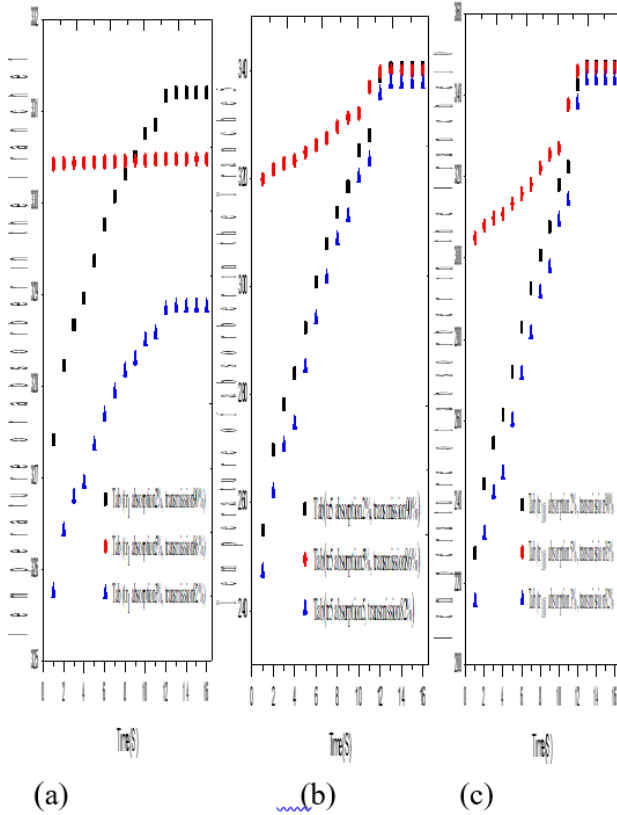
(a)   (b)   (c)

Fig.3. Evolution of the sensor absorber temperature as a function of time as the absorption rate varies

The results in Figures 4, 5 and 6 confirm those in Figures 1a, 1b and 1c. They show the effect of solar radiation on the absorption and transmission rates of the glass pane leading to its different temperature changes. The figures 4a, 4b and 4c show the variations of the different temperatures for an absorption rate of the glass of 3% and a transmission rate of 82% as a function of the radiation at the exit of the collector (last slice). The evolution of the temperatures of the different elements increases when the irradiance (500, 700, 880 W/m²) increases. We temperature of the absorber increases as the transmission coefficient of the glass increases.

This is followed by the temperature of the heat transfer fluid, which has almost the same variations as the pane at the beginning (range 1 to 3). These variations become more important when the radiation increases. Hence the temperature of the air becomes higher than that of the pane the higher the radiation. In this case the outlet temperature of the heat transfer fluid is reached at 880 W/m².
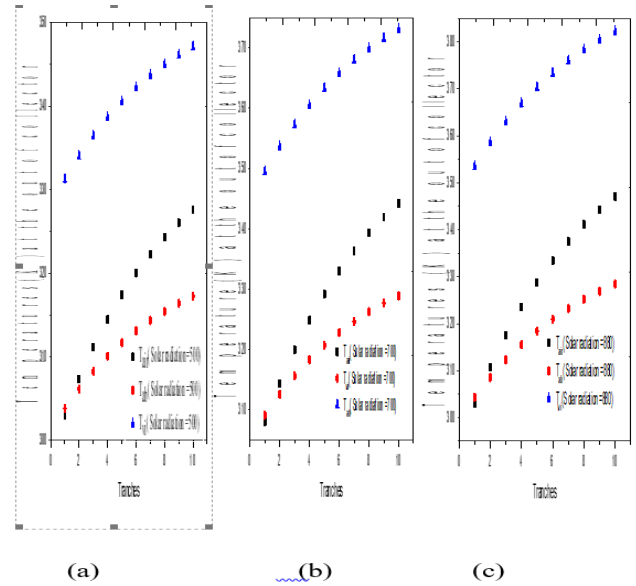

(a)   (b)   (c)

Fig.4. Temperature variations of the collector components as a function of solar radiation for a pane absorption of 3% and transmission 82%.

In figure 6 the temperature variations are the same with increasing radiation. For an absorption rate of 2% and transmission of 90%, the analysis shows the same temperature variations as in figure 5.

In this case the exit temperature of the heat transfer fluid is reached at 700 W /m² (344k after 16 hours).
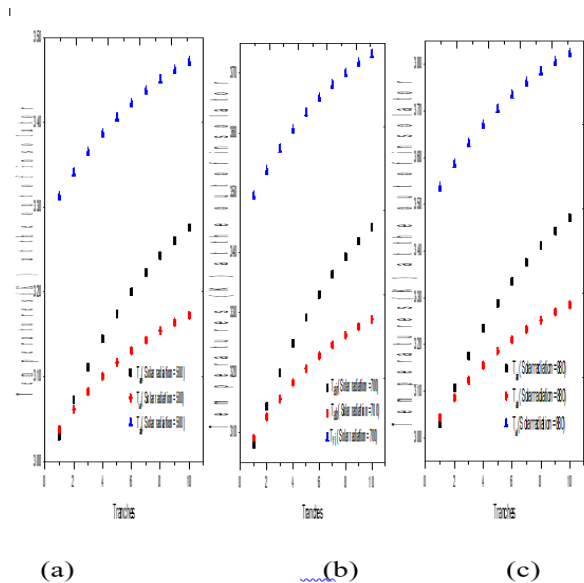

(a)   (b)   (c)

Fig.5. Temperature variations of the collector components as a function of solar radiation for a glass absorption of 2% and transmission of 90%.

As you can see in the figures above, figures 6a, b and 6c also show temperature changes as a function of radiation for an absorption coefficient of 5% and transmission of 86%. We note again the same variations as in the figures 4 and 5.

In this case the outlet temperature of the heat transfer fluid is reached at 880 W/m^2.
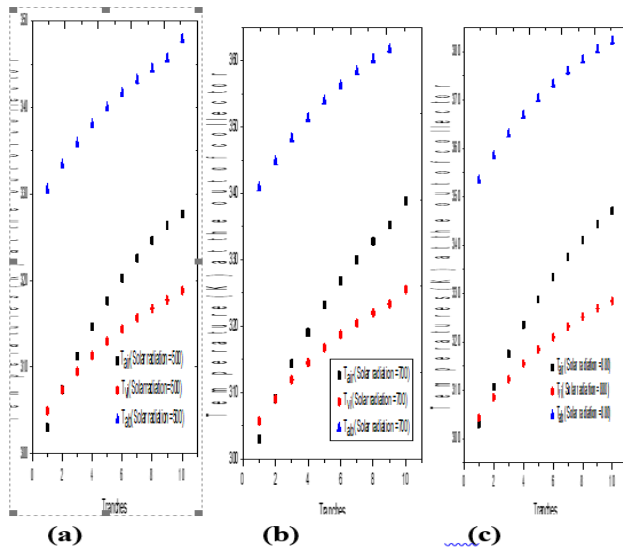

Fig.6. Temperature variations of the collector components as a function of solar radiation for 5% glass absorption and 86% transmission

According to the figures 4, 5 and 6 : the variations of the solar radiation according to time made it possible to draw the hypothesis that with a radiation of 880 W /m^2, the temperature of exit of the heat transfer fluid is obtained for the tempered glass of coefficients (3% of absorption, 82% of transmission) and the window glass of coefficients (5% of absorption to 3% and 86% of transmissions). However, for the so-called clear flat glass with coefficients (2% absorption and 90% transmission) the exit temperature is reached at a radiation of 700 W/m^2. The best choice will be a pane with a lower absorption coefficient.

IV. CONCLUSION

The numerical study undertaken in this document on the influence of radiation on the different parts of the sensor, consisted firstly, in the setting of equations. These equations are described by the heat equation applied to each element of the collector. After scaling our heat transfer equations, the spatial discretization is performed using a finite difference method while a purely implicit scheme is adopted for the temporal discretization.

In the second part, using Fortran, we wrote a numerical program giving the results. The effect of radiation on the performance of the sensor was studied by the characteristics of three types of glass. These results were used to evaluate the temperature variations of the glass, the heat transfer fluid and the absorber. The temperature of the heat transfer fluid being only that of the air leaving the collector, was obtained in this study

REFERENCES

[1]. Ammar MAOUASSI, Abdelhadi BEGHIDJA, Said DAOUD, Noureddine ZERAIBI. (2017). Etude numérique du transfert thermique à travers un capteur solaire plan en utilisant le nano fluide (TiO2/eau) comme fluide caloporteur, Colloque Interuniversitaire Franco-Québécois sur la Thermique des Systèmes.

[2]. M. Baissi1, A. Brima, N. Moummi, A. Moummi, Karoua, H. (2013). Modélisation des paramètres de fonctionnement d'un capteur solaire plan à air, Congrès Algérien de Mécanique : CAM2013, Mascara.

[3]. Mohamed Yacine NASRI, Azeddine belhamri. (2016). Simulation d'un séchoir solaire indirect a convection forcée pour les produits agroalimentaires, Sciences et Technologie B – N°44 :57-62.

[4]. Ryad BENKHELFELLAH, Sofiane El MOKRETAR, Rachid MIRI et. Maîouf BELHAME. (2005). Sechoir Solaire : Étude comparative de la cinétique de séchage des produits agroalimentaires dans des modelés de type direct et indirect, 12èmes Journées Internationales de Thermique, 259-262.

[5]. A. BOULEMTAFES and SUMMAR, D. (1999). Conception et. Réalisation d'un séchoir solaire indirect, centre de Développement des Energies Renouvelables, B.P, Alger, Rev. Energ. Ren. Valorisation Vol (6): 97 -100.

[6]. A. Ferradji, and M. Malek, and M.Bedoud, and R.Baziz, and Aoua, SA. (2001). Séchoir Solaire à Convection Forcée pour le Séchage des Fruits en Algérie, Rev. Energ. Ren. Vol (4) :49 – 59.

[7]. Daguenet,M.(1985).Les séchoirs solaires : théorie et pratique. Publication de l'UNESCO, Paris, France, pp: 320-325.

[8]. M.Kouhila, and Kane, CSE. (2006). Étude Expérimentale du Séchage convectif de la sauge dans un séchoir solaire muni d'un appoint électrique, Proceedings 1er séminaire Magrébin sur les Sciences et Technologies de Séchage, pp: 301-306.

[9]. Mamandou Seck Gueye, Omar Ngor Thiam, Samba Dia, Joseph Sarr. (2014). Description of the Temperature in an Indirect Solar Dryer: Application in the Drying of the 'Niebe' International Journal on Engineering Application (I.R.E.A), vol (2): 123-128.

[10]. Benlahmidi Said, (2013) Study of convective drying by solar energy products red, PhD Thesis, University Mohamed Khider-Biskra,

[11]. El Mokretar, R. Miri, and Belhamel, M. (2004). Energy balance and mass Study of a greenhouse type of dryer for drying applications Food products, Development Center Of Review Of Renewable Energy.Vol(7) : 41-48.

[12]. A. Boubeghal, M. Benhammou, B. Omari S. Amara L. Amer, H. Moungar and Ouejdi, S. (2007). Numerical study of a solar dryer running in natural convection, Journal of Renewable Energies ICRESD-07 Tlemcen ,pp :315 - 320.

[13]. Jean-François Rozis. (1995). Sécher des Produits Alimentaires, Techniques, Procédés, Équipements. GRET pub.

[14]. Sacadura, J.F. (1993). Initiation aux transferts thermiques. Et Doc, Lavoisier pub.

[15]. Goncalvès, E. (2005), Résolution Numérique Discrétisation des EDP et EDO, Institut National Polytechnique De Grenoble.

[16]. Euvrard, D. (1990). Résolution numérique des équations aux dérivées partielles, de la physique,de la mécanique et des sciences de l'ingénieur, différences finies, élément finies, méthode dessingularité. Masson Paris pub,2th Ed.